microRNA-204 shuttled by mesenchymal stem cell-derived exosomes inhibits the migration and invasion of non-small-cell lung cancer cells via the KLF7/AKT/HIF-1α axis

Xiao-Ni LIU[#], Chui-Bin ZHANG[#], Hai LIN, Xiao-Yuan TANG, Rong ZHOU, Hui-Lan WEN, Jie LI*

Department of Respiratory Medicine, The First Affiliated Hospital of Gannan Medical University, Ganzhou, Jiangxi, China

Correspondence: lijie31110@163.com
[#]*Contributed equally to this work.*

Non-small-cell lung cancer (NSCLC) remains the leading cause of cancer-related death worldwide. Accumulating researches have highlighted the ability of exosome-encapsulated microRNAs (miRNAs or miRs) as potential circulating biomarkers for lung cancer. The current study aimed to evaluate the significance of mesenchymal stem cells (MSCs)-derived exosomal miR-204 in the invasion, migration, and epithelial-mesenchymal transition (EMT) of NSCLC cells. Initially, the expression of miR-204 in human NSCLC tissues and cells was determined by RT-qPCR, which demonstrated that miR-204 was downregulated in NSCLC tissues and cells. Next, Krüppel-like factor 7 (KLF7) was predicted and validated to be a target of miR-204 using dual-luciferase reporter gene assay. NSCLC A549 cells were treated with MSCs-derived exosomes, after which the migration and invasion of A549 cells were detected and expression of EMT-related proteins (E-cadherin, N-cadherin, and Vimentin), KLF7, p-AKT/AKT, and HIF-1α were measured. The results of gain- and loss-of-function assays revealed that miR-204 overexpression in MSCs-derived exosomes inhibited KLF7 expression and the AKT/HIF-1α pathway activity, resulting in impaired cell migration, invasion, as well as EMT. In conclusion, the key findings of the current study demonstrate that exosomal miR-204 from MSCs possesses anticarcinogenic properties against NSCLC via the KLF7/AKT/HIF-1α axis.

Key words: non-small-cell lung cancer, mesenchymal stem cells, exosomes, microRNA-204, Krüppel-like factor 7, AKT/HIF-1α

As one of the most common types of cancers, lung cancer contributes to particularly high mortality in China, with non-small-cell lung cancer (NSCLC) accounting for the majority of lung cancer cases [1, 2]. Current therapeutic approaches for NSCLC are mainly composed of systemic therapy, radiotherapy, chemotherapy, and immunotherapy [3, 4]. More recently, mesenchymal stem cells (MSCs) have been implicated in the progression and development of multiple malignant tumors [5]. Accumulating evidence showed that MSCs mediated anti-tumor activity and inhibited the growth of tumors [6]. MSCs have been highlighted recently to have a strong exosomal secretion capacity [7]. Furthermore, exosome-encapsulated microRNAs (miRNAs) can serve as predictive biomarkers for lung cancer [8]. Thus, it is of great importance to elucidate the mechanism of exosomal miRNAs in NSCLC cells.

Exosomes act as significant cell-cell communication entities in both physiological and pathological contexts by serving as carriers of various biomolecules, including miRNAs [9]. Thus, they act as disease/cancer-specific biomarkers [10, 11]. For all the miRNA cargoes, exosomal miR-204-5p has been reported to induce apoptosis and sensitize breast cancer cells, glioma cells, lung cancer cells, and gastric cancer cells to 5-FU [12]. Additionally, miR-204 is downregulated in NSCLC cells [13]. The downregulated miR-204 is strongly correlated with poor overall survival rates in NSCLC patients [14]. Moreover, miR-204 was significantly reduced in 5-FU resistant gastric cancer cells, demonstrating mesenchymal features with declines in epithelial marker, while rises in mesenchymal markers [15], which implied the association between miR-204 and the process of epithelial-mesenchymal transition (EMT). During the current study, we utilized the Target Scan website (http://www.targetscan.org/vert_72/) to identify a relationship between miR-204 and Krüppel-like factor 7 (KLF7). KLF7 has been identified as an oncogene in NSCLC by regulating

tumorigenesis and metastasis [16]. In addition, KLF7 overexpression induced EMT and lymph node metastasis by mediating the expression of snail in oral squamous cell carcinoma [17]. Furthermore, the dysregulation of hypoxia-inducible factor-1α (HIF-1α) has been found in NSCLC cells by regulating protein kinase B (AKT) [18]. The involvement of HIF-1α, a component of HIF-1, in various cancer cells has been highlighted previously via modulating cell metastasis and tumor angiogenesis [19]. A recent study has reported the interaction between AKT and HIF-1α expression could exert great effects on the progression of NSCLC [20]. Interestingly, miR-204-5p expression was reduced in esophageal squamous cell carcinoma, and miR-204-5p repressed the development of esophageal squamous cell carcinoma by blocking the PI3K/AKT pathway [21]. Thus, we reasoned that MSCs-derived exosomes containing miR-204 could restrain NSCLC cell malignant phenotype via the KLF7/HIF-1α/AKT axis.

Patients and methods

Ethics statement. The current study was implemented with the authorization of the Ethics Committee of The First Affiliated Hospital of Gannan Medical University (Approval number: #20151109002) and based on the ethical principles for medical research involving human subjects of the *Declaration of Helsinki*. Informed written consent was collected from each participant.

Bioinformatic analysis. At first, we screened out the miRNAs with high expression in MSC-derived exosomes in the EvmicroRNA database (http://bioinfo.life.hust.edu. cn/EVmiRNA#!/) and miRNAs with poor expression in MSC-derived exosomes in the OncomiR database (http://www.oncomir.org/). The heatmap was plotted using the Venn website (http://bioinformatics.psb.ugent.be/cgi-bin/liste/Venn/). Subsequently, the KM plotter website (http://kmplot.com/analysis/index.php?p=background) predicted the survival rates of miR-204 of patients with lung adenocarcinoma (LUAD) and lung squamous cell carcinoma (LUSC) in The Cancer Genome Atlas (TCGA) database. Moreover, the binding sites of miR-204 and KLF7 were predicted through Target Scan (http://www.targetscan.org/vert_72/).

Patient enrollment. Totally 61 primary NSCLC patients (45 males and 16 females; 54.36±5.21 years old) who had received lobectomy from January 2016 to January 2018 at the First Affiliated Hospital of Gannan Medical University were enrolled in the study. None of the patients had received local or systemic radiotherapy and chemotherapy before the surgery. Resected tumor tissues and adjacent normal tissues (5 cm away from tumor tissues) were collected from each patient and immediately stored in liquid nitrogen at −80 °C. Bone marrow specimens were also collected from 5 patients (aged from 24 to 38 years) with osteonecrosis of the femoral head who were free of loss of height of the femoral head or diseases such as trauma, cardiovascular disease, or tumor. Table 1 shows the clinical stages of the NSCLC patients.

Cell culture. Normal pulmonary epithelial cell line BEAS-2B and NSCLC cells, A549, H1299, HCC2935, and ACC-LC-170 were from the Cell Bank of Shanghai Institutes for Biological Sciences, Chinese Academy of Sciences (Shanghai, China). These cells were grown in RPMI-1640 medium supplemented with 10% fetal bovine serum (FBS) and the mixture of penicillin (100 U/ml) and streptomycin (100 mg/ml) in an incubator (DHP-9162, Jie Cheng Experimental Apparatus, Shanghai, China) at 37 °C with 5% CO_2 and saturated humidity. The fresh medium was replaced every 1–2 days, and upon reaching 80% confluence, cells were sub-cultured.

Isolation and identification of human MSCs (hMSCs). First, 10 ml bone marrow was extracted from the fracture end of the femoral shaft with a 20 ml syringe (containing 2000 IU heparin) under the sterile conditions and then mixed with heparin rapidly. Bone marrow was centrifuged for 10 min at 300×g to remove the supernatant and then rinsed with Dulbecco's modified Eagle's medium (DMEM) three times. Next, the cells were subjected to incubation in 15 ml of medium, followed by the addition of the same volume of Ficoll-Paque™ lymphocyte separation solution (1.077 g/ml) for centrifugation at 900×g for 20 min. Nucleated cells were located in the interface and the upper fluid, and most of the red blood cells were deposited at the bottom. The obtained nucleated cells were washed with 30 ml phosphate buffer saline (PBS) three times, centrifuged at 300×g for 8 min, and dispersed with 5 ml cell culture medium. A total of 10 μl cell suspension was then mixed with 490 μl PBS. The cells (10 μl) were counted under the light microscope, and 1×10^5

Table 1. The clinical stages of the NSCLC patients.

Clinical information	Case (n=61)
Gender	
Male	45
Female	16
Age	
≥50	51
<50	10
Classification	
T1	17
T2	11
T3	19
T4	14
N classification	
N0	13
N1	22
N2	21
N3	5
M classification	
M0	49
M1	12

Abbreviations: NSCLC-non-small-cell lung carcinoma

cells were then inoculated in a culture bottle and cultured in 5 ml low-glucose DMEM at 37 °C with 5% CO_2 and saturated humidity. The alizarin red and oil red O were used to stain isolated hMSCs. The positive and negative markers of hMSCs were detected by flow cytometry. The positive markers were CD44 (ab264539, Abcam, Cambridge, UK), CD73 (11-0909-42, Nuowei Biotechnology Co., Ltd., Beijing, China), CD90 (MA5-17747, Thermo Fisher, Waltham, MA, USA), and CD105 (ab11414, Abcam), and negative markers were CD34 (ab54208, Abcam), CD45 (69-0459-42, Thermo Fisher, Waltham, MA, USA), CD14 (ab183322, Abcam), and CD19 (ab134114, Abcam).

Extraction and characterization of exosomes. hMSCs were subjected to centrifugation to obtain the supernatant, from which the exosomes were extracted. Briefly, conditioned medium was collected every three days and centrifuged as follows: at 300×g for 10 min to remove cells from the conditioned medium; at 2,000×g for 20 min to remove dead cells from the conditioned medium, and at 10,000×g for 30 min to remove cell debris and proteins from the conditioned medium. Finally, the supernatant was collected and filtered using a 0.22 µm filter and centrifuged at 120,000×g for 2 h. The supernatant was discarded, and the separated precipitate was precipitated with 100 µl PBS to obtain a suspension of exosomes. The bicinchoninic acid (BCA) was utilized to assess the protein concentration of exosomes, and 20 µg protein was collected for sodium dodecyl sulfate-polyacrylamide gel electrophoresis (SDS-PAGE) to measure exosome markers (CD63, CD81, TSG101, calnexin) using western blot analysis. The size distribution of exosomes was measured by Zetasizer nano ZS (Malvern Panalytical Ltd., Malvern, UK). The exosome suspension was fixed in 2% paraformaldehyde, 2.5% glutaraldehyde, and 1% osmotic acid for 1.5 h. The immobilized exosomes were subjected to dehydration with gradient ethanol, immersion in epoxy resin overnight, and then polymerization for 24 h at 60 °C. At last, the embedded vesicles, cutting into ultra-thin sections, were stained with lead and uranium salts and observed under TEM.

The specific inhibitor GW4869 (HY-19363, MCE, USA) was used to restrain exosome secretion. To confirm that miRNA was transmitted through exosomes, cells were first treated with 10 nm GW4869 or dimethyl sulfoxide (DMSO) as a control. The MSCs transfected with miR-204 were placed into a 6-well plate. The transfected MSCs were treated with GW4869 or DMSO and then co-cultured with A549 cells on a 6-well plate. After 48 h of incubation, the medium was collected to separate exosomes.

Co-culture of hMSCs-derived exosomes and NSCLC cells. A549 cells were cultured, and hMSCs were transfected with miR-204 mimic for 12 h. After that, hMSCs and A549 cells were mixed at 1:1 and then seeded in a 96-well plate (100 cells/well) for a 2-day culture. The fluorescence microscope was used for observation and photograph. Meanwhile, exosomes (20 µg) were cultured with A549 cells for a period of 48 h for the subsequent experiments.

RNA isolation and quantitation. Total RNA was isolated using TRIzol reagent (15596-026, Invitrogen, Gaithersburg, MD, USA). The optical density (OD) value and RNA concentration at 260 nm and 280 nm were measured by a nucleic acid protein analyzer (BioPhotometer D30, Eppendorf, Hamburg, Germany). The $OD_{260 nm}/OD_{280 nm}$ between 1.8–2.0 indicated the high RNA purity. Reverse transcription was conducted to synthesize complementary DNA (cDNA) using the reverse transcription Kit (K1621, Fermentas, Maryland, NY, USA). The cDNA was preserved at –20°C. Shanghai Genechem Co., Ltd. (Shanghai, China) was commissioned to design and synthesize primer sequences of miR-204, KLF7, and U6, glyceraldehyde phosphate dehydrogenase (GAPDH) (Table 2). mRNA expression was detected by fluorescence quantitative PCR kit (Takara, Dalian, China), and RT-qPCR analysis was performed in an ABI 7500 system (ABI, Foster City, CA, USA). With GAPDH or U6 serving as an internal reference, the relative expression of genes or miRNA was calculated based on relative quantification (the $2^{-\Delta\Delta Ct}$ method).

Western blot analyses. Radioimmunoprecipitation assay (RIPA) lysis buffer (R0010, Beijing Solarbio Science & Technology Co., Ltd., Beijing, China) was employed to extract total proteins or exosomes. The protein concentration was assessed through BCA kits (20201ES76, Yisheng Biotechnology Co., Ltd., Shanghai, China). After being separated by SDS-PAGE, the protein was transferred to the polyvinylidene fluoride (PVDF) membrane. After being blocked with 5% BSA for 2 h, the membrane was incubated with primary antibodies at 4°C overnight. The following diluted antibodies were used: CD63 (1:1,000; ab59479, Abcam), CD81 (1:1,000; ABP53125, AmyJet Scientific Inc., Wuhan, China), TSG101 (1:5,000; ab125011, Abcam), calnexin (1:2,000; ab92573, Abcam), E-cadherin (1:500; ABP51220, AmyJet Scientific), N-cadherin (1:5,000; 13116, Cell Signaling, Danvers, MA, USA), Vimentin (1:2,000; 5741, Cell Signaling), p-AKT (1:2,000; ab179463, Abcam), AKT (1:1,000; ab38449, Abcam), HIF-1α (1:2,000; ab2185, Abcam), KLF7 (1:5,000; ab197690, Abcam), and GAPDH (1:10,000; ab181602, Abcam). The horseradish peroxidase (HRP)-labeled goat

Table 2. Primer sequences for RT-qPCR.

Gene	Primer sequences (3'-5')
miR-204	CTGTCACTCGAGCTGCTGGAATG
	ACCGTGTCGTGGAGTCGGCAATT
KLF7	ACTGCTTGCTGACAATCTCG
	GGTCCCTCACACATCCTTCA
U6	TCTTTGGAATTCAAGGTCGGGCAGGAAGAGGGCCTA
	CGCGGATCCTAGTATATGTGCTGCCGAAGC
GAPDH	GAAGGTGAAGGTCGGAGT
	GAAGATGGTGATGGGATTTC

Abbreviations: miR-204-microRNA-204; RT-qPCR-reverse transcription quantitative polymerase chain reaction; KLF7-Krüppel-like factor 7; GAPDH-glyceraldehyde phosphate dehydrogenase

anti-rabbit IgG (1:20,000; ab150077, Abcam) secondary antibody was cultured with the membrane for 1 h and visualized by chemiluminescence (ECL). ImageJ 1.48u software (National Institutes of Health) was used for protein quantitative analysis, and the gray ratio of each protein to the internal reference GAPDH was used for protein expression analysis.

Dual-luciferase reporter gene assay. The binding sites between miR-204 and KLF7 were predicted on the website (http://www.targetscan.org/vert_72/), the results of which were further verified by dual-luciferase reporter gene assays. Reporter gene vectors of wild-type and binding site mutated (PGL3-KLF7-wt and PGL3-KLF7-mut) were constructed and transfected with miR-204 mimic or NC mimic into HEK293T cells. Twenty-four hours later, cells were centrifuged at 12,000×g for 1 min to collect the supernatant. The Dual-Luciferase® Reporter Assay System (E1910, Promega, Madison, WI, USA) was performed to detect luciferase activity. Each cell sample was added with firefly luciferase working solution (100 μl) to detect firefly luciferase activity and with Renilla luciferase working solution (100 μl) to detect Renilla luciferase activity. The ratio of firefly luciferase to Renilla luciferase was used as the relative luciferase activity.

Transwell assay for cell migration and invasion. As for the Transwell migration assay, 8 μm Transwell chambers with polycarbonate filter (Corning Incorporated, Corning, NY, USA) were used. The transfected cells (5×10⁴) were suspended in a 200 μl serum-free medium and added into the membrane of the apical chambers, and the exosomes suspended in a complete medium were added into the

basolateral chambers, followed by a 24 h culture at 37°C. Following fixation in 4% paraformaldehyde, the chambers were stained with crystal violet. The migrated cells were observed using a microscope. The number of stained cells in 10 randomly selected fields was counted on the surface of the membrane in basolateral chambers to detect cell migration. The cell invasion was detected using 8 μm Transwell chambers with 1 mg/ml Matrigel. The remaining steps were the same as in the migration assay.

Statistical analysis. The data were displayed as mean ± standard deviation, and were compared using t-test between two groups or one-way analysis of variance (ANOVA) with Bonferroni's test among multiple groups. The clinical data was tested using the χ^2 test. A value of p<0.05 was considered to be indicative of statistical significance with the help of SPSS 21.0 software (IBM Corp., Armonk, NY, USA).

Results

Decreased miR-204 expression in NSCLC contributes to the NSCLC progression. RT-qPCR validated that miR-204 expression was reduced in NSCLC tissues (p<0.05, Figure 1A), which was related to the increase of the TNM stage (Table 3). High miR-204 expression suggested a higher survival rate in NSCLC patients (Figure 1B). RT-qPCR also showed that miR-204 expression was lower in NSCLC cells relative to BEAS-2B cells, and the lowest level was observed in A549 cells (p<0.05, Figure 1C).

To investigate whether miR-204 expression could affect the NSCLC cell function, A549 cells were transfected with miR-204 mimic (with NC mimic as control) or miR-204 inhibitor (with NC inhibitor as control), respectively. RT-qPCR exhibited that miR-204 expression increased in A549 cells treated with restored miR-204 and decreased in A549 cells treated with depleted miR-204 (p<0.05, Figure 1D). Subsequently, the Transwell assay indicated that upregulated miR-204 inhibited the migration and invasion of A549 cells, whereas depleted miR-204 reversed the trends (Figures 1E, 1F). Western blot analysis clarified that E-cadherin expression elevated and expression of N-cadherin and Vimentin reduced in A549 cells after miR-204 upregulation, while the results were opposite after miR-204 depletion (p<0.05, Figure 1G). Altogether, miR-204 expression was decreased in NSCLC, and elevated miR-204 inhibited A549 cell EMT, migration, and invasion.

miR-204 targets and inhibits KLF7 expression. A binding site between miR-204 and KLF7 was predicted using Target Scan to further explore the regulatory mechanism of miR-204 in NSCLC (Figure 2A). Dual-luciferase reporter gene assay showed that luciferase activity of pGL3-KLF7-wt was significantly inhibited by miR-204 mimic (p<0.05, Figure 2B). In addition, A549 cells were transfected with miR-204 mimic (with NC mimic as control) or miR-204 inhibitor (with NC inhibitor as control), respectively. Upregulated miR-204 inhibited KLF7 mRNA and protein expres-

Table 3. Correlation of miR-204 expression and clinical data in NSCLC patients.

Clinical data	miR-204 expression	p-value
Gender		
Male	1.23±0.11	>0.05
Female	1.14±0.12	
Age		
≥50	1.13±0.16	>0.05
<50	1.19±0.23	
Classification		
T1	1.92±0.21	
T2	1.34±0.15	<0.05
T3	0.81±0.09	
T4	0.27±0.04	
N classification		
N0	1.58±0.17	
N1	0.93±0.09	< 0.05
N2	0.57±0.06	
N3	0.19±0.03	
M classification		
M0	1.47±0.16	< 0.05
M1	0.34±0.06	

Abbreviations: NSCLC-non-small-cell lung carcinoma; miR-204-microRNA-204

sion, while depleted miR-204 elevated KLF7 mRNA and protein expression (p<0.05) (Figures 2C–2E). Therefore, the obtained data suggested that miR-204 could target KLF7 and inhibit KLF7 expression.

miR-204 exerts inhibitory effects on NSCLC cells by targeting KLF7 and regulating the AKT/HIF-1α axis. A549 cells were treated with miR-204 mimic and/or vectors

containing KLF7 to explore the roles of miR-204 and KLF7 in NSCLC. The results of RT-qPCR validated that miR-204 expression increased, and KLF7 mRNA level decreased in A549 cells treated with miR-204 mimic (p<0.05). In A549 cells treated with miR-204 mimic + oe-KLF7, miR-204 expression showed no change (p>0.05) and KLF7 mRNA level was increased relative to cells transfected with miR-204 mimic and
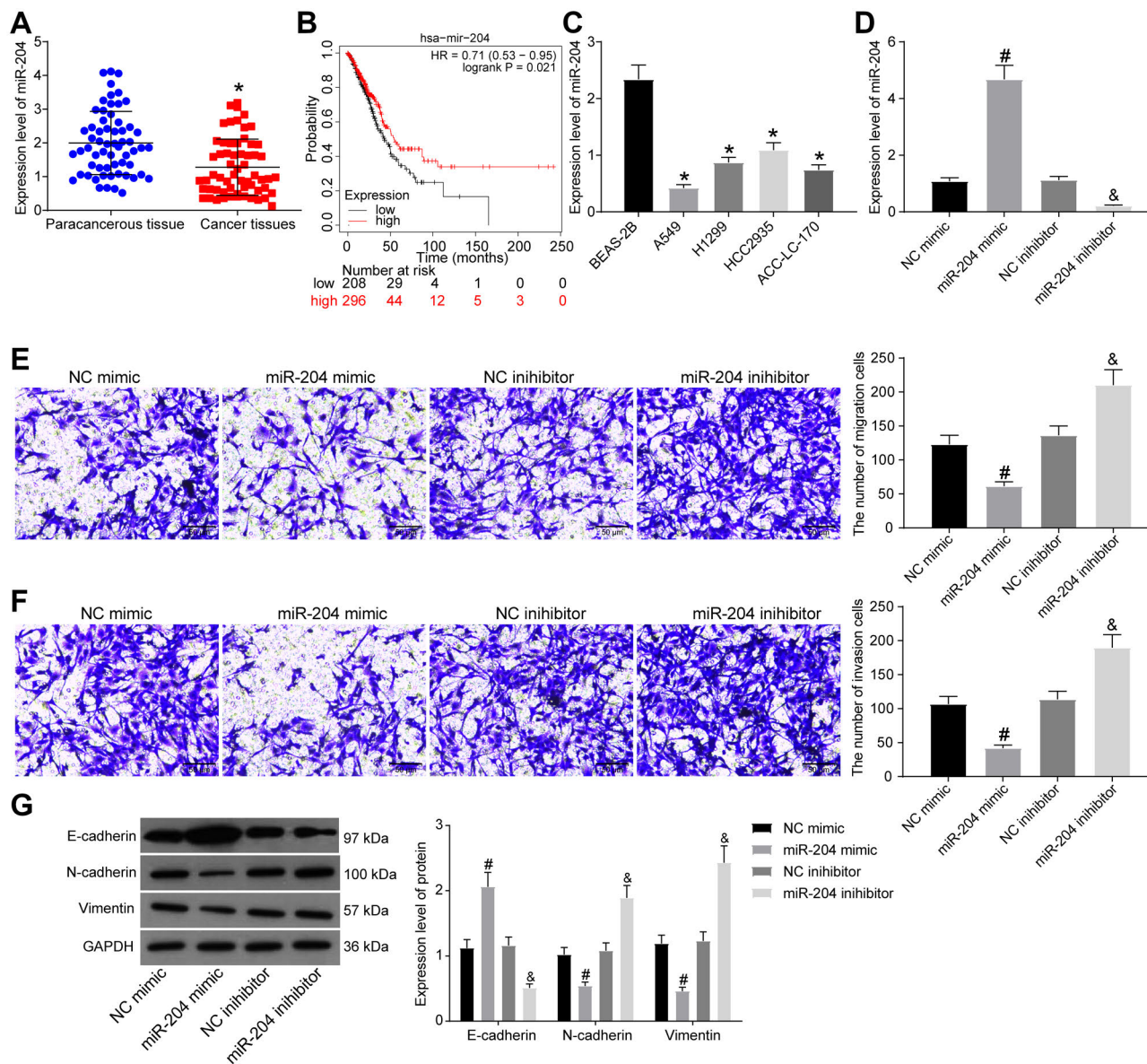

Figure 1 miR-204 is downregulated in NSCLC and upregulated miR-204 inhibits A549 cell malignant phenotype. A) miR-204 expression in NSCLC and adjacent tissues determined by RT-qPCR. B) Correlation between miR-204 and survival rate of LUAD and LUSC in TCGA predicted using the Kaplan-Meier plotter website. C) miR-204 expression in BEAS-2B, A549, H1299, HCC2935, and ACC-LC-170 cells determined by RT-qPCR. A549 cells were treated with miR-204 mimic (with NC mimic as control) and miR-204 inhibitor (with NC inhibitor as control), respectively. D) miR-204 expression after transfection in A549 cells assessed by RT-qPCR. E–F) A549 cell migration (E) and invasion (F) evaluated by Transwell assay; scale bars: 50 µm. G) Protein levels of E-cadherin, N-cadherin, and Vimentin detected by western blot analysis. *p<0.05 vs. adjacent normal tissues or BEAS-2B cells. #p<0.05 vs. A549 cells transfected with NC mimic. &p<0.05 vs. A549 cells transfected with NC inhibitor. Data (mean ± standard deviation) between two groups were compared by unpaired t-test, while data among multiple groups were compared using two-way ANOVA, followed by Bonferroni's multiple post hoc test. Each assessment was done in triplicate with 3-time repetition to ensure minimum deviation; n=61.
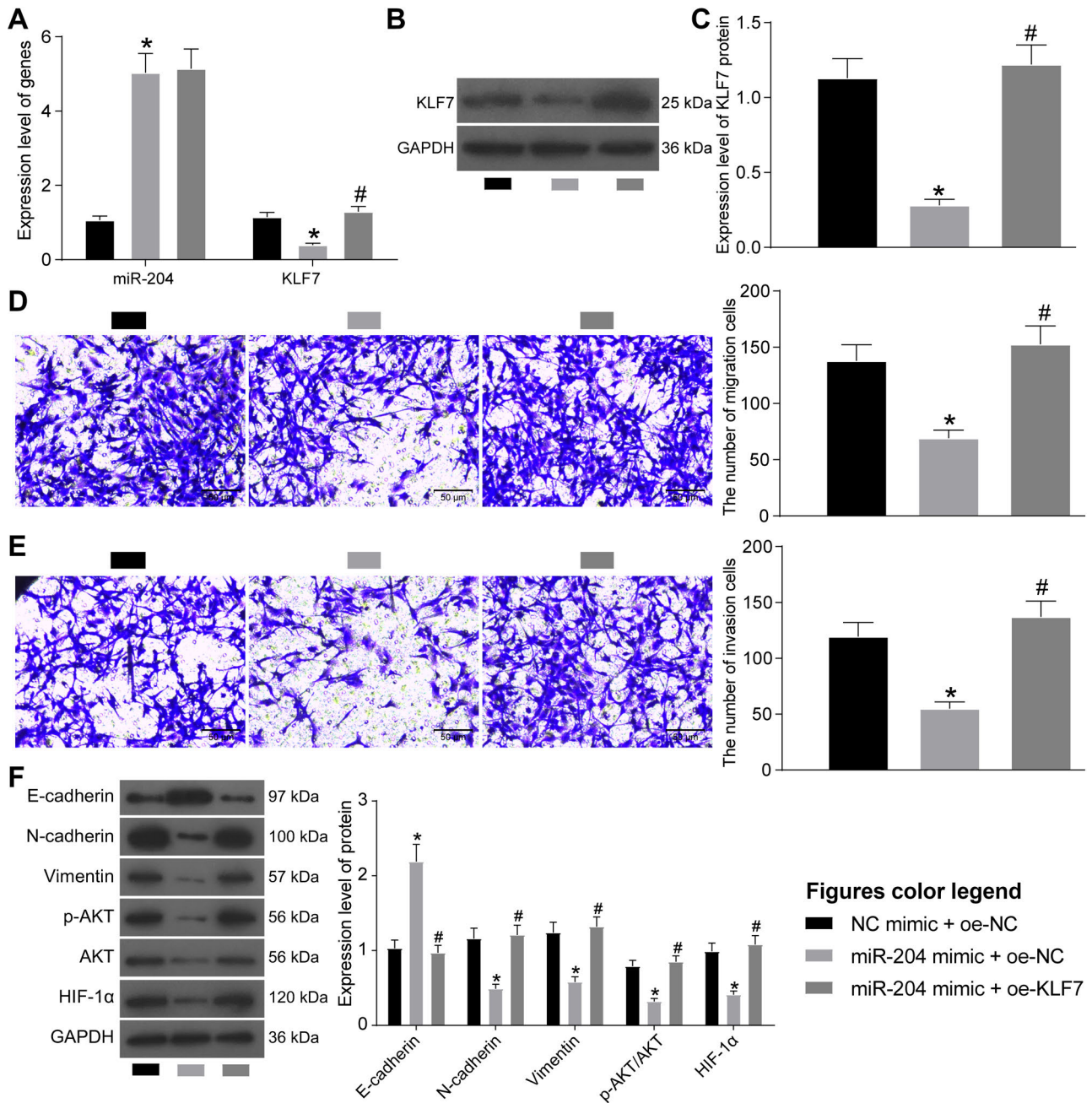
Figure 2 miR-204 could target KLF7 and suppresses KLF7 expression. A) The binding sites between miR-204 and KLF7 predicted using Target Scan. B) Target relationship between miR-204 and KLF7 detected using dual-luciferase reporter gene assay. A549 cells were treated with miR-204 mimic (with NC mimic as control) and miR-204 inhibitor (with NC inhibitor as control), respectively. C) KLF7 mRNA level in A549 cells determined by RT-qPCR. D–E) KLF7 protein band patterns (D) and protein level (E) in A549 cells detected by western blot analysis. *p<0.05 vs. A549 cells treated with NC mimic. #p<0.05 vs. A549 cells treated with NC inhibitor. Data (mean ± standard deviation) between two groups were analyzed by unpaired t-test, while data among multiple groups were analyzed using two-way ANOVA, followed by Bonferroni's multiple post hoc test. The experiment was repeated three times independently.

oe-NC (p<0.05, Figure 3A). Western blot analyses presented that KLF7 expression reduced in A549 cells treated with miR-204 mimic and elevated in A549 cells following overexpression of miR-204 and KLF7 (p<0.05, Figures 3B, 3C).

Transwell migration (Figure 3D) and Transwell invasion assay (Figure 3E) exhibited the cellular capabilities of migration and invasion were suppressed by the treatment of miR-204 mimic alone, while A549 cell migration and invasion were facilitated by the treatment of miR-204 mimic and vectors containing KLF7 (p<0.05). In addition, it has been demonstrated that KLF5 could enhance the drug resistance of NSCLC by upregulating AKT/HIF-1α expression [22]. Moreover, our western blot results revealed upregulated E-cadherin expression, along with downregulated expression of N-cadherin, Vimentin, p-AKT/AKT, and HIF-1α in cells in the presence of miR-204 mimic, and A549 cells treated with miR-204 mimic and vectors containing KLF7 exhibited the reverse trends (p<0.05, Figure 3F). Given the aforementioned findings, the tumor-suppressive effects of miR-204 on NSCLC cells and the AKT/HIF-1α axis could be restored by upregulated KLF7.

hMSCs and exosomes are successfully extracted. The highly expressed miRNAs in MSCs-derived exosomes in the

EvmicroRNA database and the poorly expressed miRNAs in LUAD in the OncomiR database were retrieved. A total of 14 miRNAs, including miR-204, were screened out (Figure 4A), which suggested that miR-204 might be derived from hMSCs-derived exosomes. To verify the source of miR-204, we isolated hMSCs and identified the expression of surface antigens by flow cytometry. The findings showed that CD44, CD73, CD90, CD105 were positive, and CD45, CD14, CD19 were negative (Figure 4B). The isolated hMSCs were cultured and induced for adipogenic differentiation. Oil red O staining identified that hMSCs underwent adipogenic differentiation (Figure 4C). In addition, hMSCs also induced osteogenic differentiation, and alizarin red staining showed that the isolated hMSCs had osteogenic differentiation potential (Figure 4D). These findings proved that hMSCs were isolated successfully.

In addition, oval-shaped membrane vesicles were found in cultured hMSCs (Figure 4E). Based on the analysis of Zetasizer nano ZS, the size distribution of exosomes produced by hMSCs was about 62 nm (Figure 4F). Moreover, the expression of CD81, CD63, and TSG101 was increased in extracted exosomes, and calnexin showed no positive expression (Figure 4G). These findings demonstrated that exosomes

Figure 3 miR-204 inhibits A549 cell malignant phenotype by downregulating the KLF7/AKT/HIF-1α axis. A549 cells were treated with miR-204 mimic and vectors containing KLF7 (with miR-204 mimic + oe-NC as control). A) KLF7 mRNA level in A549 cells determined by RT-qPCR. B) KLF7 protein band patterns in A549 cells assessed by western blot. C) KLF7 protein level in A549 cells determined by western blot. D–E) A549 cell migration (D) and invasion (E) were detected by Transwell assay; scale bars: 50 μm. F) Protein levels of E-cadherin, N-cadherin, Vimentin, p-AKT/AKT, and HIF-1α evaluated by western blot analysis. *p<0.05 vs. A549 cells treated with NC mimic + oe-NC. #p<0.05 vs. A549 cells treated with miR-204 mimic + oe-NC. Data (mean ± standard deviation) between two groups were analyzed by unpaired t-test, while data among multiple groups were analyzed using two-way ANOVA, followed by Bonferroni's multiple post hoc test. The experiment was repeated three times independently.

were successfully isolated from hMSCs. Then, we detected the expression of miR-204 in exosomes using RT-qPCR, and we found that there was a significant enrichment of miR-204 in exosomes (Figure 4H).

Exosomal miR-204 is delivered by hMSCs into A549 cells. The exosomes isolated from hMSCs were co-cultured with A549 cells to confirm whether A549 cells can take up the exosomes. Exosomes were labeled with Dil, and A549
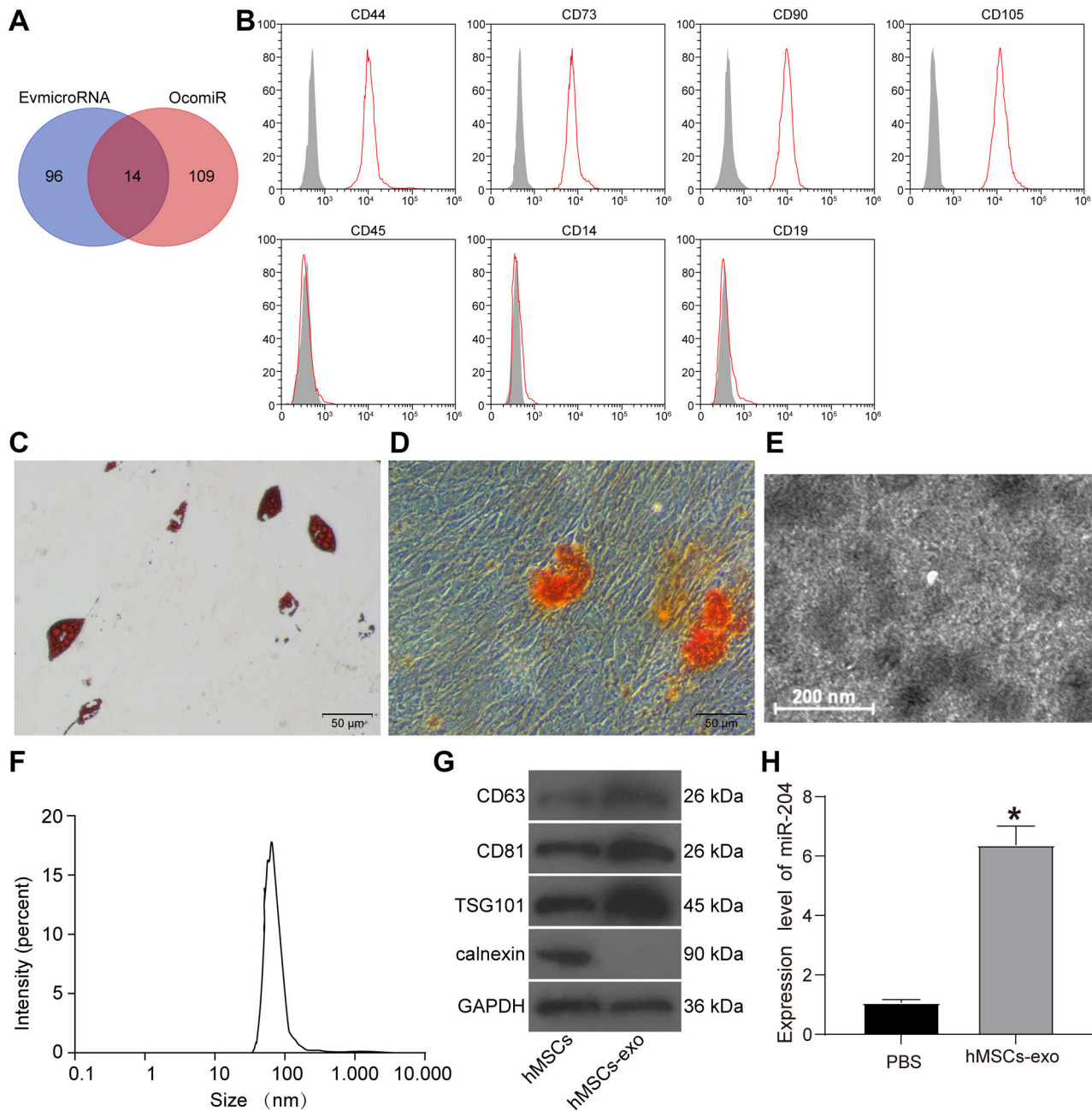
Figure 4 hMSCs and their derived exosomes were successfully isolated. A) The retrieval of the highly expressed miRNAs in MSCs-derived exosomes in the EvmicroRNA database and the poorly expressed miRNAs in LUAD in the OncomiR database. **B)** The expression of surface antigens of hMSCs was identified by flow cytometry. **C)** The adipogenic differentiation of hMSCs was detected by oil red O staining; scale bar: 50 μm. **D)** Osteogenic differentiation of hMSCs was detected alizarin red staining; scale bar: 50 μm. **E)** Morphology of exosomes under a TEM; scale bar: 200 nm. **F)** The size distribution of exosomes was detected by NTA. **G)** Representative western blots of exosome marker proteins in hMSCs. **H)** miR-204 expression in hMSCs-derived exosomes and PBS by RT-qPCR. *p<0.05 vs. PBS treatment. Data (mean ± standard deviation) between two groups were analyzed by unpaired t-test. The experiment was repeated three times independently.

cells were labeled with Hoechst. After 48 h of incubation, the uptake of exosomes by A549 cells was detected by immunofluorescence (Figure 5A), which validated that A549 cells could phagocytose exosomes. The hMSCs transfected with miR-204 mimic were co-cultured with A549 cells to confirm

that miR-204 was secreted from hMSCs-derived exosomes. First, we examined the expression of miR-204 in hMSCs-derived exosomes using RT-qPCR. We found that the expression of miR-204 was significantly increased in exosomes derived from hMSCs transfected with miR-204 mimic
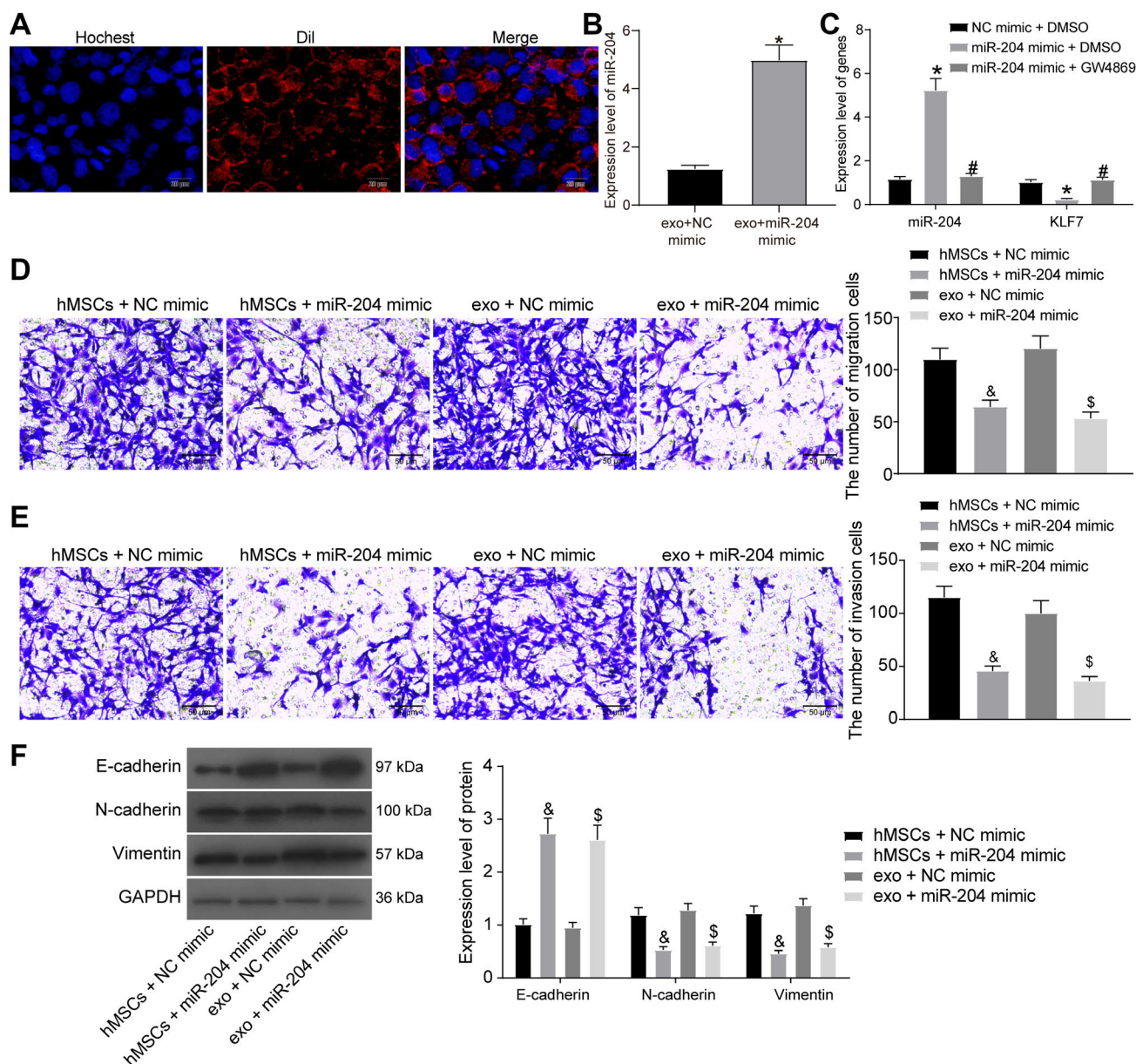
Figure 5 miR-204 can be transferred into NSCLC cells by exosomes derived from hMSCs. A549 cells were co-cultured with hMSCs transfected with miR-204 mimic or NC mimic and treated with GW4869 or DMSO. A) Uptake of exosomes in A549 cells by immunofluorescence; scale bars: 20 μm. B) miR-204 expression in hMSCs-derived exosomes by RT-qPCR. C) miR-204 expression and KLF7 mRNA level in A549 cells after co-culture determined by RT-qPCR. The hMSCs + miR-204 mimic (with hMSCs + NC mimic as control) and exo + miR-204 mimic (with exo + NC mimic as control) were co-cultured with A549 cells, respectively. D–E) A549 cell migration (D) and invasion (E) were detected by Transwell assay; scale bars: 50 μm. F) Protein levels of E-cadherin, N-cadherin, and Vimentin detected by western blot analysis. *p<0.05 vs. A549 cells co-cultured with hMSCs treated with NC mimic + DMSO or exo + NC mimic. #p<0.05 vs. A549 cells co-cultured with hMSCs treated with miR-204 mimic + DMSO. &p<0.05 vs. A549 cells co-cultured with hMSCs treated with NC mimic. $p<0.05 vs. A549 cells co-cultured with exosomes derived from hMSCs treated with NC mimic. Data (mean ± standard deviation) between two groups were analyzed by unpaired t-test, while data among multiple groups were analyzed using two-way ANOVA, followed by Bonferroni's multiple post hoc test. The experiment was repeated three times independently.

(Figure 5B). Subsequently, the exosome release was inhibited by treating the hMSCs with GW4869, and the expression of miR-204 and KLF7 mRNA in A549 cells was detected by RT-qPCR after co-culture with hMSCs (Figure 5C). The results revealed that miR-204 expression increased and KLF7 mRNA level decreased in A549 cells co-cultured with hMSCs transfected with miR-204 mimic and DMSO, while the addition of GW4869 led to lower miR-204 expression and higher KLF7 mRNA in cells (p<0.05), suggesting that hMSCs-derived exosomes carried miR-204 into A549 cells.

When A549 cells were co-cultured with hMSCs overexpressing miR-204 or hMSCs-derived exosomes, respectively, there was a significant reduction in the migration and invasion abilities of A549 cells (Figures 5D, 5E). Subsequently, we used western blot to detect the expression of EMT-related factors in A549 cells after co-culture. The expression of E-cadherin was significantly upregulated, whereas N-cadherin and Vimentin were significantly reduced in A549 cells after co-culture with hMSCs overexpressing miR-204 or hMSCs-derived exosomes (Figure 5F). Notably, the inhibitory effects on cell migration, invasion, and EMT were more pronounced in hMSCs-derived exosomes.

miR-204 inhibitor impairs the inhibitory effect of hMSCs-derived exosomes on the aggressiveness of A549 cells. To further verify the role of hMSCs-derived exosomes in inhibiting the aggressiveness of A549 cells by carrying miR-204, we transfected miR-204 inhibitor as well as the corresponding inhibitor NC into A549 cells and verified the transfection efficiency by RT-qPCR (Figure 6A). A549 cells were subsequently treated with hMSCs-derived exosomes. We found a significant increase in the expression of KLF7 in the cells after treatment with miR-204 inhibitor (Figure 6B). Subsequently, we further examined the altered cell migration and invasion abilities using Transwell assays. The inhibitory effects of hMSCs-derived exosomes on the migration and invasion of A549 cells were significantly diminished after the suppression of miR-204 expression in A549 cells (Figures 6C, 6D).

Discussion

NSCLC represents the main reason for cancer-related mortality worldwide, with an unsatisfied survival rate despite advancements in the therapies [23]. Exosomes continue
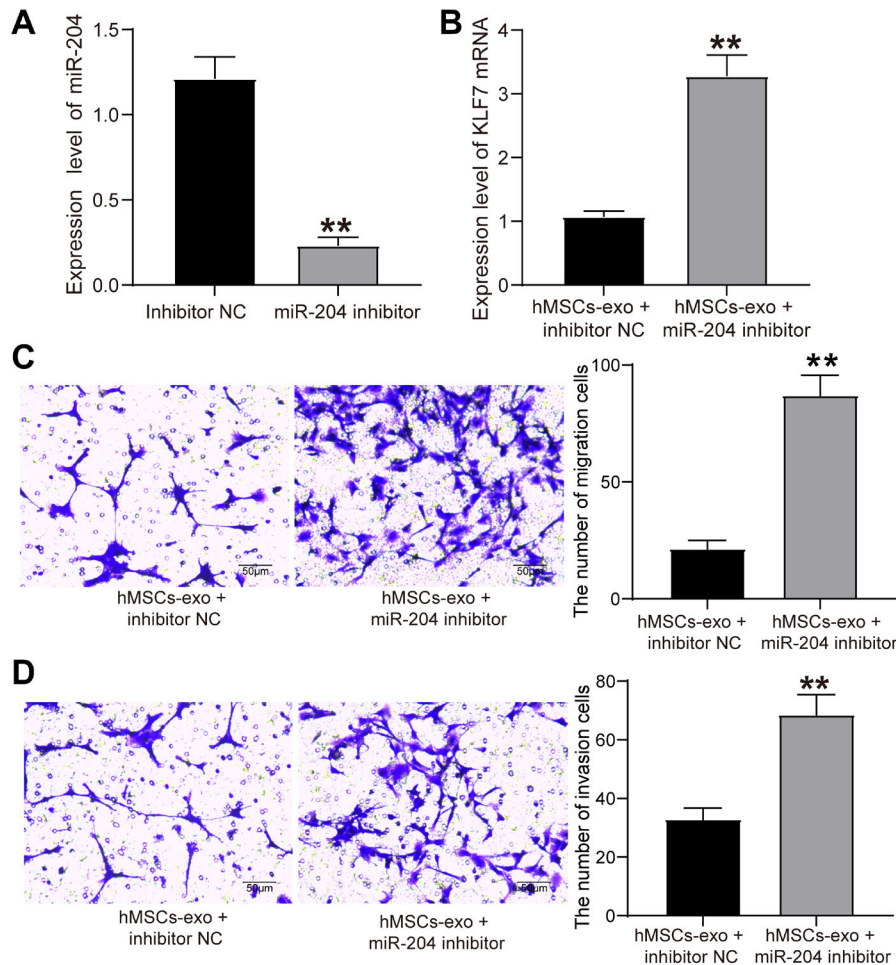

Figure 6 miR-204 inhibitor impairs the inhibitory effect of hMSCs-derived exosomes on A549 cell malignant phenotype. miR-204 inhibitor and the corresponding inhibitor NC were transfected into A549 cells. A) miR-204 expression in A549 cells after transfection by RT-qPCR. B) KLF7 mRNA level in A549 cells after transfection and co-culture determined by RT-qPCR. C-D) A549 cell migration (C) and invasion (D) were detected by Transwell assay; scale bars: 50 μm. **p<0.01 vs. A549 cells transfected with inhibitor NC or A549 cells transfected with inhibitor NC and co-transfected with hMSCs-derived exosomes. Data (mean ± standard deviation) between two groups were analyzed by unpaired t-test. The experiment was repeated three times independently.

to be an area of research interest owing to their ability to carry miRNAs and their potential as prospective diagnostic markers for lung cancer [24]. The role of miR-204 from the MSCs-derived exosome in NSCLC was explored and it was demonstrated that miR-204 from the MSCs-derived exosomes could regulate NSCLC cell malignant phenotype via the KLF7/AKT/HIF-1α axis.

Our initial observations revealed that miR-204 was poorly expressed in NSCLC, which was related to the poor survival rate of NSCLC patients. miR-204 was downregulated in various human cancers, such as liver cancer [25], head and neck squamous cell carcinoma [26], in addition to cervical cancer [27], suggesting that elevated miR-204 acts as a tumor inhibitor. As expected, overexpression of miR-204 was found to inhibit A549 cell EMT, migration, and invasion in our study. Similarly, miR-204 expression was decreased in NSCLC, and the overexpression of miR-204 inhibited the invasive and migratory capacities of NSCLC cells [13]. miR-204 downregulation was related to a higher invasion risk and poor prognosis of NSCLC sufferers, and the augmentation of miR-204 inhibited NSCLC metastasis [28]. miR-204-5p restoration also exerted a suppressive impact on the cervical cancer cell viability, invasion, migration, and EMT process [29]. Besides, miR-204 overexpression restrained cell invasion, migration, and EMT by upregulating E-cadherin and downregulating N-cadherin and Vimentin expression in gastric cancer [30], oral squamous cell carcinoma, [31] as well as NSCLC [32]. Therefore, these findings support that miR-204 could be considered as a possible biomarker to hamper NSCLC progression.

Moreover, this study demonstrated that miR-204 targeted KLF7 and miR-204 elevation consequently suppressed its expression. KLF7 was highly expressed in NSCLC, which contributed to the EMT event in NSCLC [33]. In addition, we provided evidence in the present investigation that miR-204 exerted inhibitory effects in A549 cell EMT, migration, and invasion by inhibiting KLF7 via inactivation of the AKT/HIF-1α axis. A recent study has demonstrated that KLF5 could enhance the drug resistance of NSCLC cells by upregulating the AKT/HIF-1α expression [22]. HIF-1α, upregulated in NSCLC, expedited the progression of NSCLC by facilitating cell proliferation and metastasis [18]. Qian et al. have proved that the depleted HIF-1α inhibited the NSCLC cell proliferation and invasion via the impairment of AKT [19]. The AKT pathway could elevate HIF-1α protein levels, and the extent of AKT phosphorylation was positively related to HIF-1α expression in NSCLC [20]. AKT was implicated in NSCLC by regulating cell proliferation and metastasis [34]. Moreover, enforced expression of miR-204 sensitized NSCLC cells to mitochondrial apoptosis induced by cisplatin through suppression of the caveolin-1/AKT pathway [35]. Therefore, we could conclude that overexpression of the KLF7/AKT/HIF-1α axis was correlated with the accelerated progression of NSCLC. Interestingly, adipose mesenchymal stem cell-derived exosomes upregulated the phosphorylation

of AKT and the expression of HIF-1α in HaCaT cells, thus expediting wound healing [36]. Nevertheless, the regulation of KLF7 on the AKT/HIF-1α axis has not been investigated in the current study, which awaits further validation.

Furthermore, it was confirmed that hMSCs-derived exosomes delivered miR-204 into NSCLC cells, and miR-204 encapsulated in MSCs-derived exosomes could inhibit NSCLC cell malignant phenotype. MSCs are implicated in multiple tumor-promoting processes, including EMT and metastasis [5]. More recently, a study has found that MSCs have a strong exosomal secretion capacity [7]. Exosomes are small vesicles composing of lipids, proteins, and small RNAs that can convey proteins, DNA, mRNAs, and miRNAs to surrounding cells and act as a medium for intercellular communication [37]. Interestingly, bone marrow MSCs-derived exosomes are capable of restraining NSCLC cell malignant phenotype *in vitro* and inhibiting the tumor growth *in vivo* by delivering miR-144 to NSCLC cells [38]. Exosomal miR-204-3p regulating EMT in pancreatic cancer has also been confirmed [39]. In our study, MSCs-derived exosome-shuttled miR-204 was found to suppress NSCLC progression via the mediation of the KLF7/AKT/HIF-1α axis.

Overall, this study showed that MSCs-derived exosome-encapsulated miR-204 could potentially inhibit the cell malignant phenotype in NSCLC by regulating the KLF7/AKT/HIF-1α axis, suggesting that miR-204 may be a promising biomarker for NSCLC diagnosis. Further investigation into the specific regulatory mechanisms of KLF7 on the AKT/HIF-1α axis in NSCLC will be summarized in our next study. Moreover, animals should be adopted to validate the effects of exosomal miR-204 mimic *in vivo* in future studies.

References

[1]   BOECKX B, SHAHI RB, SMEETS D, DE BRAKELEER S, DECOSTER L et al. The genomic landscape of nonsmall cell lung carcinoma in never smokers. Int J Cancer 2020; 146: 3207–3218. https://doi.org/10.1002/ijc.32797

[2]   ZHOU C. Lung cancer molecular epidemiology in China: recent trends. Transl Lung Cancer Res 2014; 3: 270–279. https://doi.org/10.3978/j.issn.2218-6751.2014.09.01

[3]   LI W, YU H. Separating or combining immune checkpoint inhibitors (ICIs) and radiotherapy in the treatment of NSCLC brain metastases. J Cancer Res Clin Oncol 2020; 146: 137–152. https://doi.org/10.1007/s00432-019-03094-9

[4]   REBUZZI SE, ALFIERI R, LA MONICA S, MINARI R, PETRONINI PG et al. Combination of EGFR-TKIs and chemotherapy in advanced EGFR mutated NSCLC: Review of the literature and future perspectives. Crit Rev Oncol Hematol 2020; 146: 102820. https://doi.org/10.1016/j.critrev-onc.2019.102820

[5]   TIMANER M, TSAI KK, SHAKED Y. The multifaceted role of mesenchymal stem cells in cancer. Semin Cancer Biol 2020; 60: 225–237. https://doi.org/10.1016/j.semcancer.2019.06.003

[6]   LIU L, ZHANG SX, LIAO W, FARHOODI HP, WONG CW et al. Mechanoresponsive stem cells to target cancer metastases through biophysical cues. Sci Transl Med 2017; 9. https://doi.org/10.1126/scitranslmed.aan2966

[7]   ZHAO G, GE Y, ZHANG C, ZHANG L, XU J et al. Progress of Mesenchymal Stem Cell-Derived Exosomes in Tissue Repair. Curr Pharm Des 2020; 26: 2022–2037. https://doi.org/10.2174/1381612826666200420144805

[8]   FUJITA Y, KUWANO K, OCHIYA T, TAKESHITA F. The impact of extracellular vesicle-encapsulated circulating microRNAs in lung cancer research. Biomed Res Int 2014; 2014: 486413. https://doi.org/10.1155/2014/486413

[9]   WALKER S, BUSATTO S, PHAM A, TIAN M, SUH A et al. Extracellular vesicle-based drug delivery systems for cancer treatment. Theranostics 2019; 9: 8001–8017. https://doi.org/10.7150/thno.37097

[10] COUTO N, CAJA S, MAIA J, STRANO MORAES MC, COSTA-SILVA B. Exosomes as emerging players in cancer biology. Biochimie 2018; 155: 2–10. https://doi.org/10.1016/j.biochi.2018.03.006

[11] ZHOU S, HU T, ZHANG F, TANG D, LI D et al. Integrated Microfluidic Device for Accurate Extracellular Vesicle Quantification and Protein Markers Analysis Directly from Human Whole Blood. Anal Chem 2020; 92: 1574–1581.

[12] YAO S, YIN Y, JIN G, LI D, LI M et al. Exosome-mediated delivery of miR-204-5p inhibits tumor growth and chemoresistance. Cancer Med 2020. https://doi.org/10.1002/cam4.3248

[13] WANG P, LV HY, ZHOU DM, ZHANG EN. miR-204 suppresses non-small-cell lung carcinoma (NSCLC) invasion and migration by targeting JAK2. Genet Mol Res 2016; 15. https://doi.org/10.4238/gmr.15026415

[14] ZHANG S, GAO L, THAKUR A, SHI P, LIU F et al. miRNA-204 suppresses human non-small cell lung cancer by targeting ATF2. Tumour Biol 2016; 37: 11177–11186. https://doi.org/10.1007/s13277-016-4906-4

[15] LI LQ, PAN D, CHEN Q, ZHANG SW, XIE DY et al. Sensitization of Gastric Cancer Cells to 5-FU by MicroRNA-204 Through Targeting the TGFBR2-Mediated Epithelial to Mesenchymal Transition. Cell Physiol Biochem 2018; 47: 1533–1545. https://doi.org/10.1159/000490871

[16] AN YX, SHANG YJ, XU ZW, ZHANG QC, WANG Z et al. STAT3-induced long noncoding RNA LINC00668 promotes migration and invasion of non-small cell lung cancer via the miR-193a/KLF7 axis. Biomed Pharmacother 2019; 116: 109023. https://doi.org/10.1016/j.biopha.2019.109023

[17] DING X, WANG X, GONG Y, RUAN H, SUN Y et al. KLF7 overexpression in human oral squamous cell carcinoma promotes migration and epithelial-mesenchymal transition. Oncol Lett 2017; 13: 2281–2289. https://doi.org/10.3892/ol.2017.5734

[18] WAN J, WU W, CHEN Y, KANG N, ZHANG R. Insufficient radiofrequency ablation promotes the growth of non-small cell lung cancer cells through PI3K/Akt/HIF-1alpha signals. Acta Biochim Biophys Sin (Shanghai) 2016; 48: 371–377. https://doi.org/10.1093/abbs/gmw005

[19] QIAN J, BAI H, GAO Z, DONG YU, PEI J et al. Downregulation of HIF-1alpha inhibits the proliferation and invasion of non-small cell lung cancer NCI-H157 cells. Oncol Lett 2016; 11: 1738–1744. https://doi.org/10.3892/ol.2016.4150

[20] STEGEMAN H, SPAN PN, PEETERS WJ, VERHEIJEN MM, GRENMAN R et al. Interaction between hypoxia, AKT and HIF-1 signaling in HNSCC and NSCLC: implications for future treatment strategies. Future Sci OA 2016; 2: FSO84. https://doi.org/10.4155/fso.15.84

[21] SHEN Z, CHAI T, LUO F, LIU Z, XU H et al. Loss of miR-204-5p Promotes Tumor Proliferation, Migration, and Invasion Through Targeting YWHAZ/PI3K/AKT Pathway in Esophageal Squamous Cell Carcinoma. Onco Targets Ther 2020; 13: 4679–4690. https://doi.org/10.2147/OTT.S243215

[22] GONG T, CUI L, WANG H, WANG H, HAN N. Knockdown of KLF5 suppresses hypoxia-induced resistance to cisplatin in NSCLC cells by regulating HIF-1alpha-dependent glycolysis through inactivation of the PI3K/Akt/mTOR pathway. J Transl Med 2018; 16: 164. https://doi.org/10.1186/s12967-018-1543-2

[23] KARUPPASAMY R, VEERAPPAPILLAI S, MAITI S, SHIN WH, KIHARA D. Current progress and future perspectives of polypharmacology: From the view of non-small cell lung cancer. Semin Cancer Biol 2019. https://doi.org/10.1016/j.semcancer.2019.10.019

[24] LIN J, WANG Y, ZOU YQ, CHEN X, HUANG B et al. Differential miRNA expression in pleural effusions derived from extracellular vesicles of patients with lung cancer, pulmonary tuberculosis, or pneumonia. Tumour Biol 2016. https://doi.org/10.1007/s13277-016-5410-6

[25] YU Y, WANG Y, XIAO X, CHENG W, HU L et al. MiR-204 inhibits hepatocellular cancer drug resistance and metastasis through targeting NUAK1. Biochem Cell Biol 2019; 97: 563–570. https://doi.org/10.1139/bcb-2018-0354

[26] ZHUANG Z, YU P, XIE N, WU Y, LIU H et al. MicroRNA-204-5p is a tumor suppressor and potential therapeutic target in head and neck squamous cell carcinoma. Theranostics 2020; 10: 1433–1453. https://doi.org/10.7150/thno.38507

[27] DUAN S, WU A, CHEN Z, YANG Y, LIU L et al. miR-204 Regulates Cell Proliferation and Invasion by Targeting EphB2 in Human Cervical Cancer. Oncol Res 2018; 26: 713–723. https://doi.org/10.3727/096504017X15016337254641

[28] SHI L, ZHANG B, SUN X, LU S, LIU Z et al. MiR-204 inhibits human NSCLC metastasis through suppression of NUAK1. Br J Cancer 2014; 111: 2316–2327. https://doi.org/10.1038/bjc.2014.580

[29] ZHANG P, HOU Q, YUE Q. MiR-204-5p/TFAP2A feedback loop positively regulates the proliferation, migration, invasion and EMT process in cervical cancer. Cancer Biomark 2020. https://doi.org/10.3233/CBM-191064

[30] LIANG Y, ZHANG CD, ZHANG C, DAI DQ. DLX6-AS1/miR-204-5p/OCT1 positive feedback loop promotes tumor progression and epithelial-mesenchymal transition in gastric cancer. Gastric Cancer 2020; 23: 212–227. https://doi.org/10.1007/s10120-019-01002-1

[31] TAN X, ZHOU C, LIANG Y, LAI YF, LIANG Y. Circ_0001971 regulates oral squamous cell carcinoma progression and chemosensitivity by targeting miR-194/miR-204 in vitro and in vivo. Eur Rev Med Pharmacol Sci 2020; 24: 2470–2481. https://doi.org/10.26355/eurrev_202003_20515

[32] XIA Y, ZHU Y, MA T, PAN C, WANG J et al. miR-204 functions as a tumor suppressor by regulating SIX1 in NSCLC. FEBS Lett 2014; 588: 3703–3712. https://doi.org/10.1016/j.febslet.2014.08.016

[33] ZHAO L, ZHANG Y, LIU J, YIN W, JIN D et al. miR-185 Inhibits the Proliferation and Invasion of Non-Small Cell Lung Cancer by Targeting KLF7. Oncol Res 2019; 27: 1015–1023. https://doi.org/10.3727/096504018X15247341491655

[34] YANG WB, ZHANG WP, SHI JL, WANG JW. MiR-4299 suppresses non-small cell lung cancer cell proliferation, migration and invasion through modulating PTEN/AKT/PI3K pathway. Eur Rev Med Pharmacol Sci 2018; 22: 3408–3414. https://doi.org/10.26355/eurrev_201806_15163

[35] HUANG G, LOU T, PAN J, YE Z, YIN Z et al. MiR-204 reduces cisplatin resistance in non-small cell lung cancer through suppression of the caveolin-1/AKT/Bad pathway. Aging (Albany NY) 2019; 11: 2138–2150. https://doi.org/10.18632/aging.101907

[36] ZHANG Y, HAN F, GU L, JI P, YANG X et al. Adipose mesenchymal stem cell exosomes promote wound healing through accelerated keratinocyte migration and proliferation by activating the AKT/HIF-1alpha axis. J Mol Histol 2020. https://doi.org/10.1007/s10735-020-09887-4

[37] LIU S, ZHAN Y, LUO J, FENG J, LU J et al. Roles of exosomes in the carcinogenesis and clinical therapy of non-small cell lung cancer. Biomed Pharmacother 2019; 111: 338–346. https://doi.org/10.1016/j.biopha.2018.12.088

[38] LIANG Y, ZHANG D, LI L, XIN T, ZHAO Y et al. Exosomal microRNA-144 from bone marrow-derived mesenchymal stem cells inhibits the progression of non-small cell lung cancer by targeting CCNE1 and CCNE2. Stem Cell Res Ther 2020; 11: 87. https://doi.org/10.1186/s13287-020-1580-7

[39] SONOHARA F, YAMADA S, TAKEDA S, HAYASHI M, SUENAGA M et al. Exploration of Exosomal Micro RNA Biomarkers Related to Epithelial-to-Mesenchymal Transition in Pancreatic Cancer. Anticancer Res 2020; 40: 1843–1853. https://doi.org/10.21873/anticanres.14138